ACS Catalysis

Research Article

pubs.acs.org/acscatalysis

Room Temperature Activation of Oxygen by Monodispersed Metal Nanoparticles: Oxidative Dehydrogenative Coupling of Anilines for Azobenzene Syntheses

Shuangfei Cai,[†] Hongpan Rong,[†] Xiaofei Yu,[†] Xiangwen Liu,[†] Dingsheng Wang,[†] Wei He,*[,‡] and Yadong Li*[,†]

[†]Department of Chemistry and [‡]Tsinghua-Peking Joint Center for Life Science, Tsinghua University, Beijing, 100084, People's Republic of China

Supporting Information

ABSTRACT: It is highly challenging but desirable to develop efficient catalysts for the activation of oxygen under mild conditions. Here, we report that various monodispersed metal nanoparticles (Ag, Pt, Co, Cu, Ni, Pd, and Au) efficiently activated molecular oxygen under mild conditions, illustrated by the aerobic oxidation of anilines to form either symmetric or asymmetric aromatic azo compounds. This discovery indicates that exploiting the catalytic power of nanoparticles could enable sustainable chemistry suitable for important oxidation reactions.

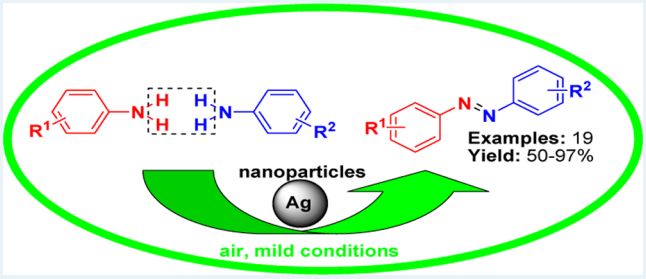

KEYWORDS: *nanoparticle, oxygen activation, oxidation coupling, azobenzene*

1. INTRODUCTION

Oxidation reactions are of fundamental importance in nature. Catalytic oxidations that use oxygen as green oxidants in organic synthesis are of the utmost significance.[1] To develop efficient catalysts for activation of oxygen is highly challenging but desirable.[2−4] Metal nanoparticles (NPs) are implicated in many industrial reactions, predominantly in heterogeneous catalysis; for instance, oxidation,[5−9] olefin polymerization,[10] desulfurization,[11] ammonia synthesis,[12] and so on. For their ubiquitous role, research on metal nanoparticle catalysis has been a central focus and has witnessed tremendous progresses.[13−15] On one hand, much effort has been dedicated to probing the mechanistic profile, partially enabled by advancements in synthetic methodology[16] and characterization techniques.[17] On the other hand, exploiting their catalytic power in new types of transformations serves as an avenue to meet the urgent demand of sustainable development.[18] One important front is oxidation reactions utilizing molecular oxygen as the green oxidant.[19] A prominent example is the Au NPs/metal oxides catalyst reported by Haruta and co-workers[20] for low-temperature CO oxidation. Recently, Corma and co-workers[21] in their seminal contribution described an inspiring Au NPs/TiO_2 catalyst that enabled the first catalytic synthesis of aromatic azo compounds. In this regard, a generally applicable, recyclable catalyst that activates oxygen at room temperature under atmospheric pressure is likely to impact many important oxidation reactions both in the laboratory and in industry.

Monodispersed metal NPs,[22] which combine the advantages of both homogeneous and heterogeneous catalysts, including facile access to reactant molecules as well as easy separation and recycling of the catalysts, are emerging as one of the most promising novel catalyst classes.[23] Recently, we have developed a systemic synthetic technique for monodispersed metal NPs.[24−26] In our effort to probe their advantages in catalysis based on the above rationale, we discovered that many types of metal NPs could efficiently activate molecular oxygen in air at room temperature, leading to the synthesis of azo compounds via oxidative coupling of anilines.

Aromatic azo compounds have found important applications in many industry sectors ranging from dyes, pigments, and food additives to pharmaceuticals.[27−31] Reflecting their oxidation state, azo compounds are most conveniently accessed by oxidative coupling of anilines. Classic methods entail stoichiometric reactions that employ 1 or more molar equivalents of environmentally unfriendly oxidants, such as Mn, Pb, and Hg salts.[32−34] In light of the sustainable chemistry, catalytic dehydrogenative coupling of anilines using molecular oxygen as the oxidant not only is attractive but also has met with some exciting successes.[21,35] Notably, unsymmetric aromatic azo compounds are typically obtained through the coupling reaction of aryl diazonium salt with electrophilic aromatics[36−38] or the Mills reaction.[39,40] There is currently a lack of a generally applicable catalyst that is capable of oxidative coupling of aniline under mild conditions. It is in this context that we wish to report the discovery of such a catalyst: Ag/C

Received: November 1, 2012
Revised: January 6, 2013
Published: February 4, 2013

   dx.doi.org/10.1021/cs300707y | ACS Catal. 2013, 3, 478−486

(12.4 nm). We demonstrate that it is highly selective, efficient, and recyclable for the syntheses of both symmetric and unsymmetrical azobenzenes, featuring air as the sole oxidant under mild conditions.

2. RESULTS AND DISCUSSION

2.1. Catalyst Preparation. Monodispersed Ag NPs were obtained by the reduction of $AgNO_3$ in nontoxic octadecylamine (ODA) according to the protocol described in ref 24. Here, ODA acts as solvent, reducing agent, and surfactant. By changing the reaction temperature and reaction time, various Ag NPs with different sizes were synthesized. Ag/C catalysts were conveniently prepared by an impregnation method.

Other monodispersed NPs were prepared as follows. Pd NPs were obtained by the reduction of palladium(II) acetyl acetonate in ODA by a procedure similar to that described above. Au NPs were prepared by the reduction of $HAuCl_4{\cdot}4H_2O$ in a solution containing oleylamine (OA) and oleic acid. Pt, Ni, Cu, and Co NPs were obtained by the reduction of the corresponding acetyl acetonate-based metal precursors in OA or a solution containing toluene and OA in the presence of borane-*tert*-butylamine complex (TBAB).

2.2. Catalyst Characterization. The morphology and size of the as-prepared NPs were examined by transmission electron microscopy (TEM). The as-prepared Ag NPs with average sizes of 7.7, 9.4, 12.4, and 25.3 nm were composed of spherical particles (Figure 1).

The 12.4 nm Ag NPs can be well supported on carbon by standard impregnation methods. Figure 2a and 2b show that the obtained Ag/C catalysts consist of spherical particles of unchanged average particle size (12.4 nm). The ICP result shows that the content of Ag in the 12.4 nm Ag/C sample was 3.2 wt %.

The TEM images and the particle size distribution of various as-prepared Pt, Co, Cu, Ni, Pd, and Au NPs are shown in Figure 3.

2.3. Catalyst Activity. We detected the formation of azobenzene when attempting Ag NPs synthesis using aniline as the growth inhibition agent. We thus quickly identified that aniline could be converted into azobenzene in moderate yield in the presence of a catalytic amount of Ag NPs in DMSO under air. Interestingly, no product was detected in the absence of Ag NPs. In addition, no product was detected when the reaction was carried out under a nitrogen atmosphere. This serendipitous discovery suggested a catalytic oxidative coupling of aniline, featuring metal NPs as the catalyst and molecular oxygen as the oxidant. On the basis of this hypothesis, we screened various metal NPs. To our great delight, monodispersed Ag, Pt, Co, Cu, Ni, Pd, and Au NPs were found to be active at room temperature under air (Table 1). This general yet high activity, possibly arising from the metal NPs' intrinsic size-/shape-dependent properties, represents the "magic" power of NPs in chemical reactions.

We sought to understand the general activity of the NPs by probing their catalytic behavior and, in turn, to query their advantage as the catalyst in azobenzene synthesis. To this end, we chose Ag NPs (12.4 nm) as a model catalyst because of their higher activity, convenient syntheses, and reactivity.

The key to the process is the activation of molecular oxygen in air. We found that Ag NPs is critical to the generation of superoxide anion radical (Figure 4a, top) using electron spin resonance (ESR) because no superoxide radical anion was detected in the absence of Ag NPs (Figure 4a, bottom).

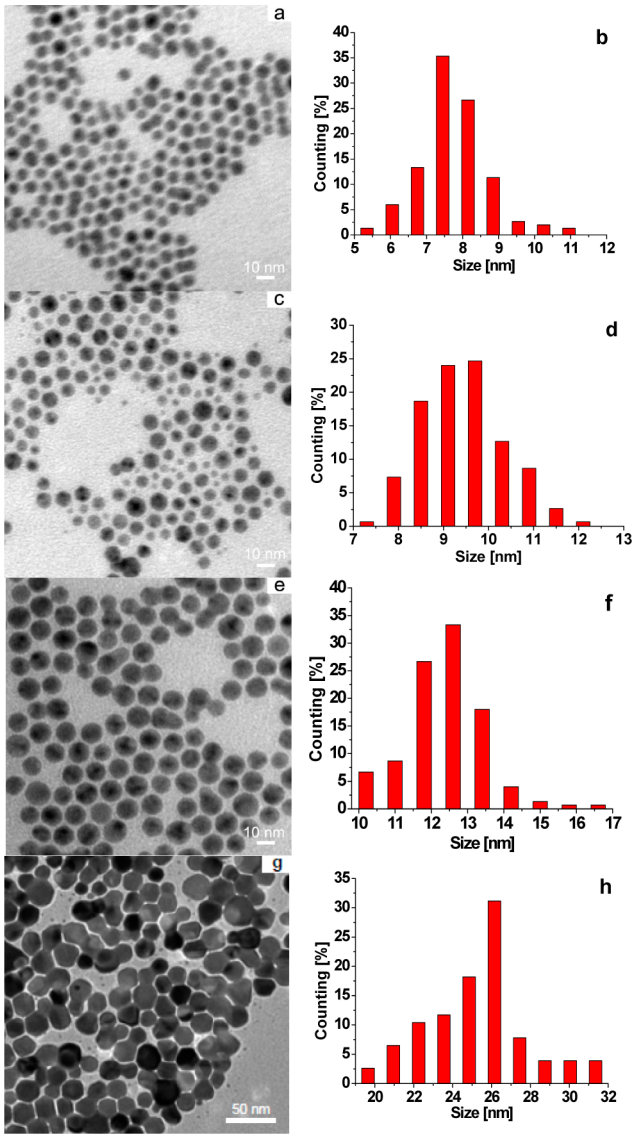

Figure 1. TEM images and the particle size distributions of Ag NPs with average particle diameter d = 7.7 (a, b), 9.4 (c, d), 12.4 (e, f), and 25.3 nm (g, h).

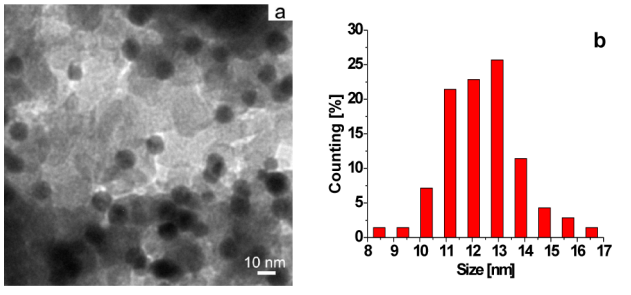

Figure 2. TEM image and the particle size distribution of Ag/C with average Ag particle diameter d = 12.4 nm.

Further, we identified the presence of aniline radical cation intermediate (Figure 4b) together with superoxide radical anion (asterisked, Figure 4b) by in situ ESR. No aniline radical cation intermediate was observed in the absence of Ag NPs (not shown). This evidence suggested that Ag NPs catalyzed the

dx.doi.org/10.1021/cs300707y | ACS Catal. 2013, 3, 478−486

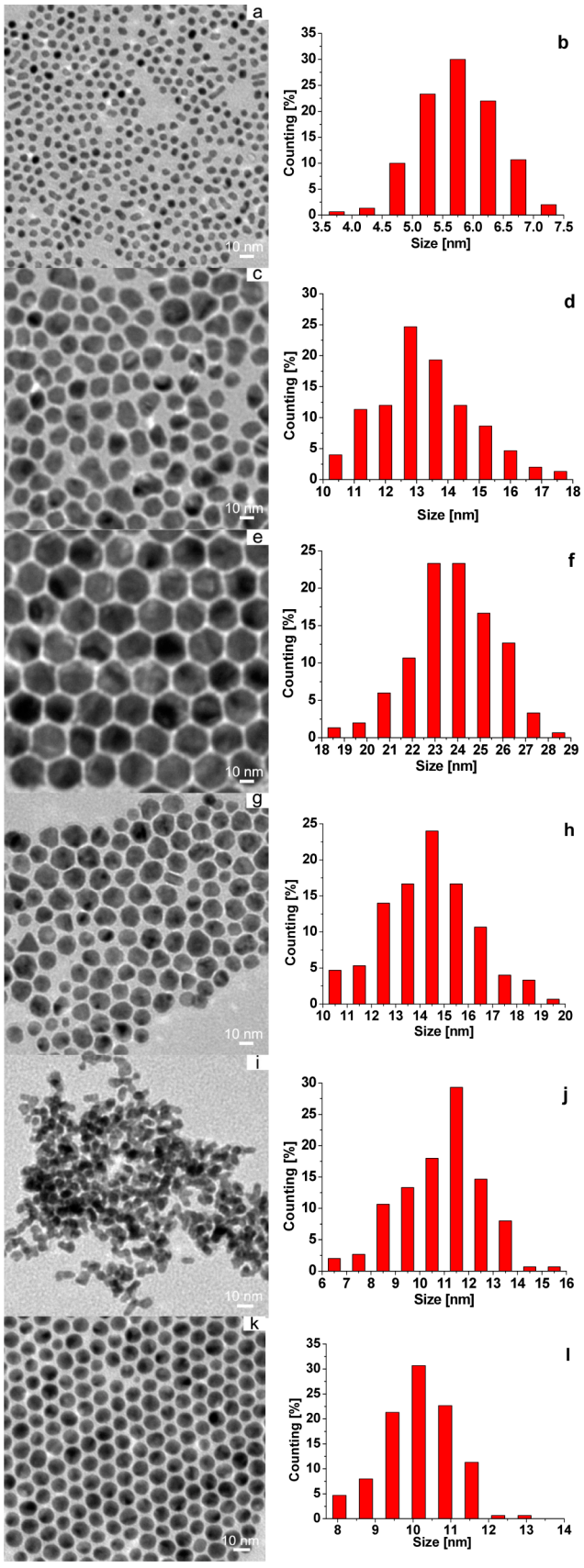

Figure 3. TEM images and the particle size distributions of 5.7 nm Pt (a, b), 13.3 nm Co (c, d), 23.9 nm Cu (e, f), 14.4 nm Ni (g, h), 10.9 nm Pd (i, j), and 10.1 nm Au (k, l) NPs.

Table 1. Oxidative Coupling of Aniline with Different Metal NPs[a]

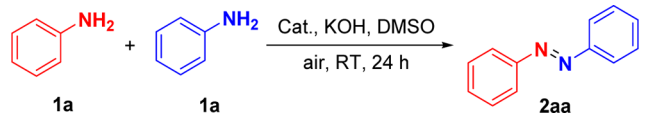

1a 1a 2aa

entry	catalyst	size/nm	yield/%[b]
1	Ag NPs	12.4	58
2	Pt NPs	5.7	46
3	Co NPs	13.3	45
4	Cu NPs	23.9	28
5	Ni NPs	14.4	42
6	Pd NPs	10.9	52
7	Au NPs	10.1	38

[a]Standard reaction conditions: **1a** (1 mmol), KOH (1 equiv), metal NPs (1 mol %), DMSO (2 mL), air (1 atm), RT, 24 h. [b]Isolated yields.

formation of an aniline radical cation intermediate through the superoxide anion radical.

To further elucidate the NPs role in the reaction, we studied the size effect of Ag NPs. To this end, Ag NPs with average sizes ranging from 7.7, 9.4 to 25.3 nm were examined under standard conditions (Table 2). There is no significant difference in the activities of the first two catalysts at 1 mol % loading (entries 1 and 2, Table 2), in accordance with the result obtained by Ag NPs of 12.4 nm. When the average size of the Ag NPs increased to 25.3 nm, however, the reaction rate decreased drastically (entry 3, Table 2). These observations substantiated that the surface area is critical to the adsorption and activation of molecular oxygen and the success of the reaction is largely dependent on the NPs' ability to activate oxygen.

To probe the reaction mechanism, several control experiments were carried out. Only a trace amount of product was obtained when the reaction was performed under N_2, underscoring the participation of dioxygen in the reaction (eq 1). We also established that nitrosobenzene was not a viable

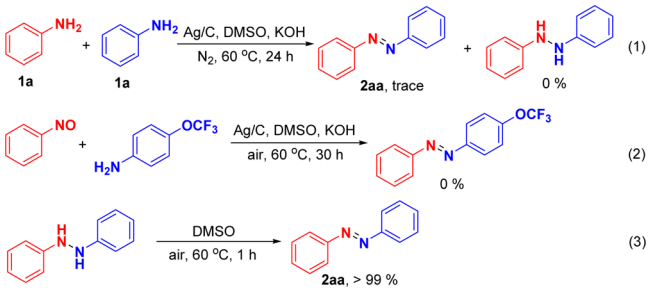

intermediate for this reaction because no crossover product was observed, as indicated by eq 2. We further discovered that hydrazine was oxidized rapidly into the azo product (eq 3), which explains the fact that we did not detect any hydrazine intermediate during the course of the reaction.

On the basis of the above evidence, we postulated the reaction mechanism (Scheme 1).[21] Oxidation of the nitrogen atom of aniline **1a** by **A** gave rise to aniline radical cation **B**. Subsequent coupling between **B** and an aniline molecule probably led to the formation of a three-electron σ bond in intermediate **C**, which was the rate-limiting step of the overall reaction, evident by the accumulation of aniline radical cation **B**

dx.doi.org/10.1021/cs300707y | ACS Catal. 2013, 3, 478−486

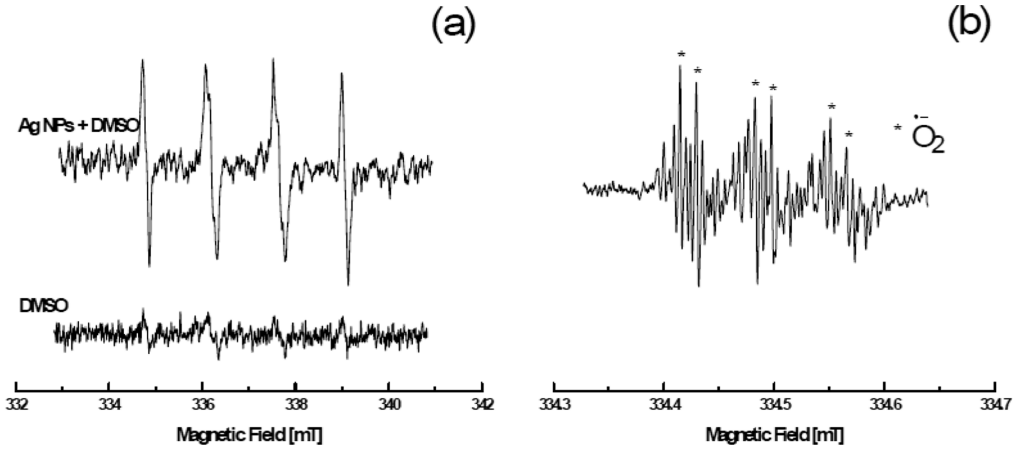

Figure 4. ESR spectra of (a) superoxide anion (g = 2.0020, a^{N} = 1.45 mT, a^{H} = 1.40 mT, $a^{H\alpha}$ = 1.40 mT, and $a^{H\beta}$ = 0.08 mT) obtained from a mixture of Ag NPs (5 μmol), DMSO (2 mL), and spin trap DMPO (6 μmol) and (b) the mixture of Ag NPs (5 μmol), aniline (1 mmol), KOH (0.5 equiv), DMSO (2 mL), and spin trap NBP (15 mg). The spectra showed the superposed signal of superoxide anion and aniline free radical cation during the reaction course.

Table 2. Particle Size Effect on the Catalyst Performance[a]

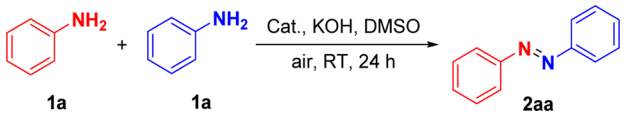

entry	size/nm	yield/%[b]
1	7.7	61
2	9.4	59
3	25.3	31

[a]Standard reaction conditions: **1a** (1 mmol), KOH (1 equiv), Ag NPs (1 mol %), DMSO (2 mL), air (1 atm), RT, 24 h. [b]Isolated yields.

Table 3. Catalyst Loading and Recycle Experiments[a]

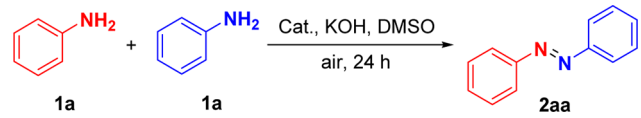

entry	catalyst	temp./°C	yield/%[b]
1	Ag NPs	25	51
2	Ag NPs	40	78
3	Ag NPs	60	97
4	Ag/C	25	55
5	Ag/C	40	81
6	Ag/C	60	97
7	Ag/C	110	95
8	reused Ag/C cycle 2	60	94
9	reused Ag/C cycle 3	60	94
10	reused Ag/C cycle 4	60	94
11	reused Ag/C cycle 5	60	93

[a]Standard reaction conditions: **1a** (1 mmol), KOH (1 equiv), Ag NPs (6 mol ‰), DMSO (2 mL), air (1 atm), 24 h. [b]Isolated yields.

observed by the ESR experiment. In addition, one-electron oxidation of intermediate **C** led to hydrazine intermediate **D**, which was rapidly oxidized to the azo product **2aa**.

The high activity of Ag NPs in oxygen activation necessitates very low catalyst loading (Table 3). Thus, 6 mol ‰ Ag NPs was capable of effecting the reaction at room temperature in 24 h in 51% yield (entry 1, Table 3). At 40 °C (entry 2, Table 3) and 60 °C (entry 3, Table 3), the reaction proceeded faster to give 78% and 97% yields, respectively. In fact, this facile activation of oxygen by the Ag NPs was successfully applied to the catalytic oxidation of N−H or C−H bond(s) to form C−N, C−O, C═C, and C═N bonds, which will be reported elsewhere in detail because of space restraints.

Scheme 1. The Proposed Mechanism for Ag NPs-Catalyzed Oxidative Coupling of Aniline

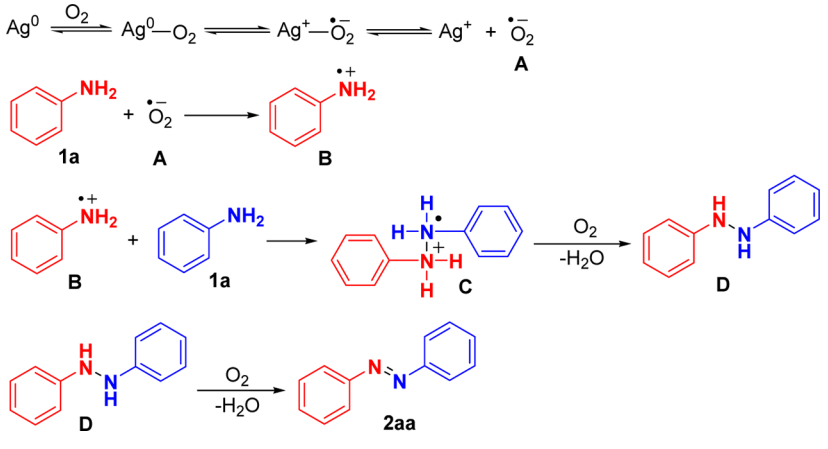

dx.doi.org/10.1021/cs300707y | ACS Catal. 2013, 3, 478−486

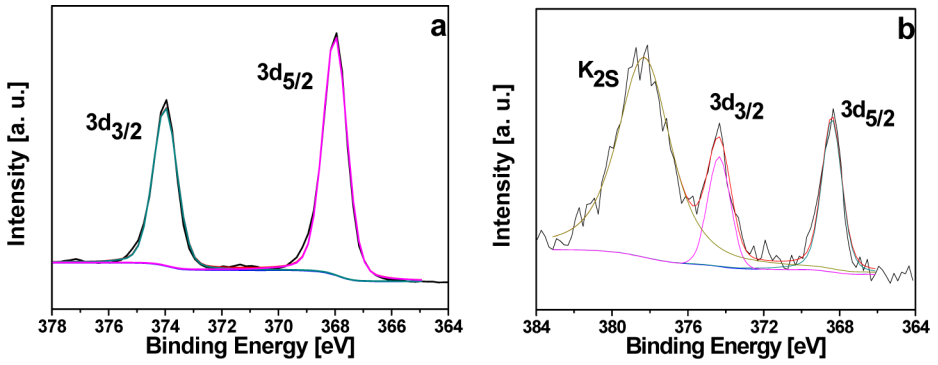

Figure 5. XPS spectrum of catalyst: (a) the fresh Ag/C and (b) a catalyst sample taken during the reaction course (contaminated by KOH).

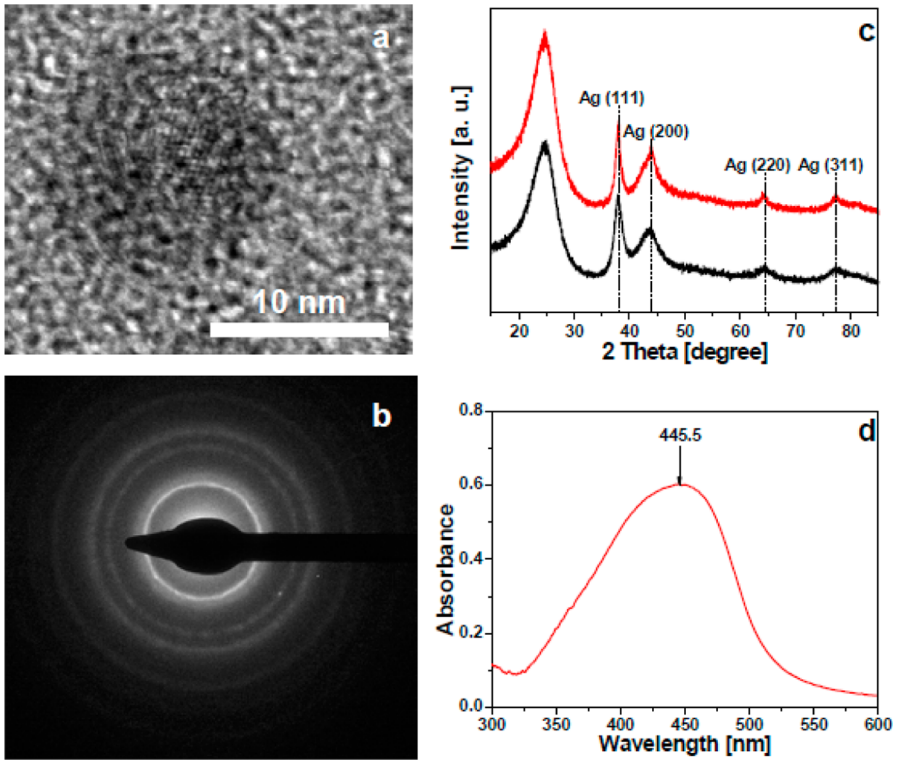

Figure 6. Characterization of catalyst: (a) HRTEM image of a catalyst sample taken during the reaction course and (b) the corresponding SAED pattern; (c) XRD patterns of the fresh Ag/C (red line) and a catalyst sample taken during the reaction course (black line); (d) UV−vis spectra of the fresh Ag nanoparticles.

Notably, the activity of our Ag/C catalysts of 12.4 nm (entries 4−6, Table 3) is very similar to that of unsupported Ag NPs of 12.4 nm (entries 1−3, Table 3) despite the reaction temperature. The results showed that the solid support was unlikely to play a role in the activation of molecular oxygen, indicating that the NPs, but not the support, was responsible for oxygen activation. Importantly, the Ag/C catalyst can be recycled and reused for several cycles by simple filtration with no loss in catalytic activity (entries 8−11, Table 3). After the fifth cycle of reaction, the Ag concentration in the filtrate was found to be 0.001 mg/mL (6 ‰ of the total amount of Ag in the reaction mixture), which is consistent with the good recyclability of the Ag/C catalyst. Further reaction carried out with the filtrate did not result in any detectable amount of azobenzene. These results suggested that the reaction was catalyzed by Ag NPs, but not the leached Ag ions.

To shed light on the active catalytic species as well as the recyclability of the Ag/C, we carried out XPS, HRTEM, SAED, XRD, and UV−vis experiments to further characterize the catalyst. XPS experiments[41,42] were carried out with the fresh Ag/C catalyst and with a Ag/C sample taken during the reaction course. The results showed that the fresh catalyst (Figure 5a) was composed of Ag^0. Figure 5b suggested that the catalyst was not oxidized during the reaction course.

High resolution transmission electron microscopy (HRTEM) was performed on a catalyst sample taken during the reaction course (Figure 6a). Figure 6b shows the corresponding selected area electron diffraction (SAED) pattern. The electron diffraction rings obtained with the same sample could be indexed to the (111), (200), (220), and (311) planes of face-centered cubic Ag.[43] It also revealed the polycrystalline structure of the catalyst, which could also be seen from the HRTEM.

The XRD pattern was obtained with a catalyst sample taken during the reaction course and compared with that of the fresh Ag/C (Figure 6c). The XRD patterns of both samples exhibited

dx.doi.org/10.1021/cs300707y | ACS Catal. 2013, 3, 478−486

diffraction peaks at 2θ = 37.9, 43.9, 64.3, and 77.3°, representing (111), (200), (220), and (311) planes of Ag nanoparticles, respectively.[44,45]

In accordance with XPS observation, this evidence indicated that the oxidation state of the Ag/C catalyst did not change during the reaction course.

UV−vis spectroscopy of the fresh Ag nanoparticles showed an absorption band at 445.5 nm that could be assigned to Ag nanoparticles (Figure 6d), close to literature reported values of characteristic Ag^0.[45−47] Because of the interference of the active carbon support, however, we failed to obtain results of any Ag/C sample.

2.4. Reaction Scope. We reasoned that anilines should have minimum influence on the reaction outcome because Ag NPs' high reactivity in oxygen activation would lead to sufficiently fast generation of aniline radical cation. We thus tested various anilines with different substitutions. As shown in Table 4, they could all be smoothly converted into the corresponding symmetric azobenzenes. Although the literature indicates that the electron density of the aniline was essential to the fate of the reaction,[21,35] the Ag NPs catalyst clearly overcame such an influence.

Table 4. Symmetric Aromatic Azo Compounds under Standard Conditions[a]

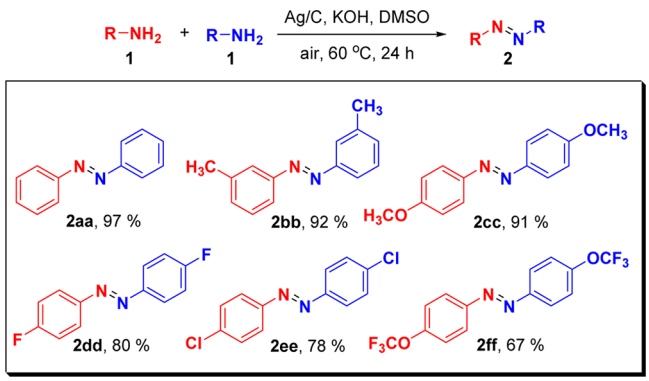

[a]Standard reaction conditions: **1** (1 mmol), KOH (1 equiv), Ag/C (6 mol‰), DMSO (2 mL), air (1 atm), 60 °C, 24 h. Isolated yields.

We envisioned that cross-coupling of anilines would become practical because the Ag NPs catalyst discriminated anilines to very little extent. Oxidative cross-coupling between anilines was problematic because the homocoupling of the more reactive aniline (electron-rich) usually prevailed. A large excess of the less reactive (electron-poor) anilines was used to achieve cross-coupling at the cost of atomic economy and purification. With Ag NPs catalyst, we needed to use only 1-fold excess of the less reactive anilines to give very good yields of the desired asymmetric azobenzenes (Table 5). Clearly, the metal NPs' power in oxygen activation has significantly improved the reaction selectivity and atomic economy.

3. CONCLUSIONS

In summary, we discovered that monodispersed metal NPs can activate O_2 in air at room temperature and under atmospheric pressure, exemplified in the sustainable syntheses of both symmetric and asymmetric azobenzenes under mild conditions. By virtue of high reactivity originating from their microstructures, we demonstrated their generality in metal sources, high efficiency, recyclability, and atomic economy. More importantly, their unprecedented ability in oxygen activation might facilitate other important oxidation reactions that have been awaiting sustainable methods. Indeed, research in our laboratories has successfully harnessed their power in oxygen activation for oxidative C−N, C−O, C═C, and C═N bond formation reactions utilizing molecular oxygen as the green oxidant. We envision that intensified investigation would open a new chapter of research that brings more reactions to the benefit of metal nanoparticle catalysis.[48]

4. EXPERIMENTAL SECTION

Preparation of 7.7 nm Ag NPs. In a typical synthesis of 7.7 nm Ag NPs, 0.034 g of $AgNO_3$ was added into 1.5 g of ODA at 90 °C, then the resulting solution was injected into 6 g of ODA at 210 °C under vigorous stirring. After stirring for 5 min, the product was precipitated by ethanol and collected by subsequent centrifugation. The precipitate was then washed by ethanol several times, and the final product was dispersed in cyclohexane for further use.

Preparation of 9.4 nm Ag NPs. In a typical synthesis of 9.4 nm Ag NPs, 0.034 g of $AgNO_3$ was added into 1.5 g of ODA at 90 °C, then the resulting colorless and clear solution was injected into 6 g of ODA at 210 °C under vigorous stirring. After stirring for 7 min, the product was precipitated by ethanol and collected by subsequent centrifugation. The precipitate was then washed by ethanol several times, and the final product was dispersed in cyclohexane for further use.

Preparation of 12.4 nm Ag NPs. In a typical synthesis of 12.4 nm Ag NPs, 0.034 g of $AgNO_3$ was added into 1.5 g of ODA at 80 °C. The resulting colorless and clear solution was injected into 6 g of ODA at 200 °C under vigorous stirring. After stirring for 10 min, the product was precipitated by ethanol and collected by subsequent centrifugation. The precipitate was washed by ethanol several times, and the final product was dispersed in cyclohexane for further use.

Preparation of 25.3 nm Ag NPs. In a typical synthesis of 25.3 nm Ag NPs, 0.0085 g of $AgNO_3$ was added into 1.5 g of ODA at 80 °C. The resulting colorless and clear solution was injected into 5.5 g of ODA at 200 °C under vigorous stirring. After stirring for 10 min, the product was precipitated by ethanol and collected by subsequent centrifugation. The precipitate was washed by ethanol several times, and the final product was dispersed in cyclohexane for further use.

Preparation of 12.4 nm Ag/C catalysts. In a typical synthesis of 12.4 nm Ag/C catalyst, 200 mg of charcoal was dispersed in cyclohexane and stirred with ultrasound for 1 h. After cooling to room temperature, the solution of the as-prepared 12.4 nm Ag NPs (10 mg) dispersed in cyclohexane was added and mixed, then the slurry was stirred for 24 h and cyclohexane was removed under reduced pressure.

Preparation of Au NPs. In a typical synthesis of Au NPs, 0.02 g of $HAuCl_4{\cdot}4H_2O$ was added into 5 mL of OA and 2 mL of oleic acid, then the solution was stirred for 20 min at 140 °C and then allowed to cool to room temperature. After washing with ethanol several times, the final product was dispersed in cyclohexane.

Preparation of Pt or Ni NPs. In a typical synthesis of Pt or Ni NPs, 0.01 g of platinum(II) acetyl acetonate or nickel(II) acetyl acetonate was added into 5 mL of OA. Under stirring, 0.03 g of TBAB was put into the above system, and then the solution was transferred into a Teflon cup in a stainless steel-lined autoclave. The autoclave was maintained at 150 °C for 2 h and then allowed to cool to room temperature. After washing

dx.doi.org/10.1021/cs300707y | ACS Catal. 2013, 3, 478−486

Table 5. Asymmetric Aromatic Azo Compounds under Standard Conditions[a]

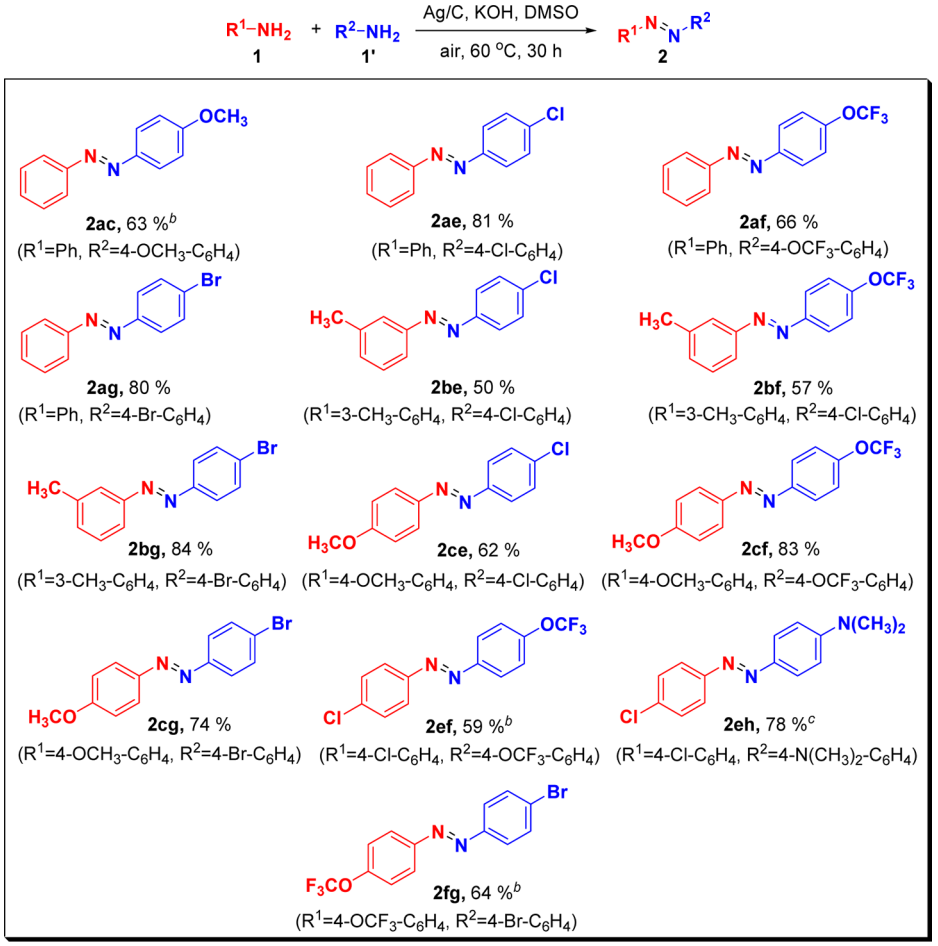

[a]Standard reaction conditions: R^1–NH_2 (0.5 mmol), KOH (2 equiv), R^2–NH_2 (0.9 mmol), catalyst loading (6 mol ‰), DMSO (2 mL), air (1 atm), 60 °C, 30 h. Isolated yields. [b]R^1–NH_2 (0.5 mmol), R^2–NH_2 (0.5 mmol). [c]R^1–NH_2 (0.9 mmol), R^2–NH_2 (0.5 mmol).

with ethanol several times, the final product was dispersed in cyclohexane.

Preparation of Cu or Co NPs. In a typical synthesis of Cu or Co NPs, 0.01 g of copper(II) acetyl acetonate or cobalt(II) acetyl acetonate was added into a solution containing 10 mL of toluene and 0.5 mL of OA. Under stirring, 0.03 g of TBAB was put into the above system, and then the solution was transferred into a Teflon cup in a stainless steel-lined autoclave. The autoclave was maintained at 150 °C for 10 h and then allowed to cool to room temperature. After being washed with ethanol several times, the final product was dispersed in cyclohexane.

Preparation of Pd NPs. In a typical synthesis of Pd NPs, palladium(II) acetyl acetonate (0.043 g) was added into 1.5 g of ODA at 80 °C. The resulting light yellow and clear solution was injected into 6 g of ODA at 180 °C under vigorous stirring. After stirring for 1.5 min, the product was precipitated by ethanol and collected by subsequent centrifugation, then the precipitate was washed by ethanol several times, and the final product was dispersed in cyclohexane.

Catalytic Experiment. Oxidation reaction of aniline was carried out in a glass reactor with a water-cooled reflux head under air (1 atm). For each reaction, a mixture of reactants, catalyst, base, and solvent was placed into the reactor. The reaction mixture was vigorously stirred at the designed temperature for the required time. After cooling to room temperature, the mixture was purified by flash chromatography or preparative chromatography on a silica gel. The yields of azo compounds were calculated with reference to products obtained. Product identification was carried out using ^1H and ^{13}C NMR, MS or HRMS, FT-IR, and UV–vis spectra.

Analysis. ^1H and ^{13}C NMR spectra were recorded in $CDCl_3$ on a Bruker Avance 400 MHz spectrometer with a 5 mm PABBO BB-1H/D Z-GRD Z108618/0394 multinuclear probe at 298 K. ESI spectra were recorded with an Esquire-LC ion-trap mass spectrometer equipped with an ESI source (Bruker Daltronik, Bremen, Germany). Samples were injected with a syringe pump (Cole-Parmer Instrument Company). High resolution mass spectra (HRMS) of compounds were recorded with a Fourier transform ion cyclotron resonance mass spectrometer (Bruker Apex IV). IR spectra were measured on KBr pellets with a Perkin-Elmer Spectrum One FT-IR spectrometer in the range 4000–500 cm^{-1}. UV–vis spectra were recorded in the wavelength range 200–600 nm using a Shimadzu UV-2100S recording spectrometer. GC chromatography was performed on SP-6890 with a FID detector equipped with a capillary column (SE-54, 30 m × 0.50 μm × 0.53 mm). Parameters were as follows: initial oven temperature, 60 °C, 3 min; ramp, 15 °C/min; final temperature, 260 °C; final time, 10 min; injector temperature, 260 °C; detector temperature, 250 °C; injection volume, 1 μL. ESR spectra were recorded at room temperature on a JEOL JES-FA200 ESR spectrometer

dx.doi.org/10.1021/cs300707y | ACS Catal. 2013, 3, 478–486

operating at 9.44 GHz. Typical spectrometer parameters were scan range, 100 G; field set, 3373.91 G; time constant, 30 ms; scan time, 4 min; modulation amplitude, 1 G; modulation frequency, 100 kHz; receiver gain, 1.00×10^3; microwave power, 4 mW. DMPO (5,5,-dimethyl-1-pyrroline *N*-oxide) and NBP (*N*-*tert*-butyl-α-phenylnitrone) were employed as the radical traps. TEM observation was performed on a Hitachi model H-800 transmission electron microscope (JEM 2010F, JEOL) operated at 80 kV. TEM specimens were prepared via the following procedure: The samples were dispersed in cyclohexane with the aid of 10 min ultrasonic vibration. Then a drop of the solution was transferred onto a standard holey carbon-covered-copper TEM micro grid. The metal contents of the various NPs were measured by inductively coupled plasma (ICP). Powder X-ray diffraction patterns of all the products obtained in this work were recorded with a Bruker D8-Advance X-ray powder diffractometer with monochromatized Cu Kα radiation (λ = 1.5406 Å). X-ray photoelectron spectroscopy experiments were performed on a ULVAC PHI Quantera microprobe. Binding energies (BE) were calibrated by setting the measured BE of C1s to 284.8 eV. HRTEMs were recorded by a JEOL-2010F high-resolution transmission electron microscope.

■ ASSOCIATED CONTENT

Supporting Information

Characterization of products. This material is available free of charge via the Internet at http://pubs.acs.org.

■ AUTHOR INFORMATION

Corresponding Author

*Phone: +86-10-6277 2491. Fax: +86-10-6278 8765. E-mail: (W.H.) whe@mail.tsinghua.edu.cn; (Y.L.) ydli@mail.tsinghua.edu.cn.

Notes

The authors declare no competing financial interest.

■ ACKNOWLEDGMENTS

This work was supported by the State Key Project of Fundamental Research for Nanoscience and Nanotechnology (2011CB932401 and 2011CBA00500), the National Natural Science Foundation of China (Grant No. 20921001 and 21131004), and China Postdoctoral Science Foundation (2011M500293). W. He gratefully acknowledges financial support from the Tsinghua-Peking Joint Center for Life Science and the National Key Basic Research Program of China (2012CB224802). The authors thank the senior engineer Zhanping Li for his XPS analysis.

■ REFERENCES

(1) Punniyamurthy, T.; Velusamy, S.; Iqbal, J. *Chem. Rev.* **2005**, *105*, 2329−2363.

(2) Wu, W.; Jiang, H. *Acc. Chem. Res.* **2012**, *45*, 1736−1748.

(3) *Catalytic Activation of Dioxygen by Metal Complexes*; Simandi, L. I., Ed.; Kluwer Academic Publishers: Dordrecht, The Netherlands, 1992.

(4) *The Activation of Dioxygen and Homogeneous Catalytic Oxidation*; Barton, D. H. R., Martell, A. E., Sawyer, D. T., Eds.; Plenum: New York, 1993.

(5) Kesavan, L.; Tiruvalam, R.; Rahim, M. H. A.; Saiman, M. I. B.; Enache, D. I.; Jenkins, R. L.; Dimitratos, N.; Lopez-Sanchez, J. A.; Taylor, S. H.; Knight, D. W.; Kiely, C. J.; Hutchings, G. J. *Science* **2011**, *331*, 195−199.

(6) Enache, D. I.; Edwards, J. K.; Landon, P.; Solsona-Espriu, B.; Carley, A. F.; Herzing, A. A.; Watanabe, M.; Kiely, C. J.; Knight, D. W.; Hutchings, G. J. *Science* **2006**, *311*, 362−365.

(7) Liu, Y.; Tsunoyama, H.; Akita, T.; Xie, S.; Tsukuda, T. *ACS Catal.* **2011**, *1*, 2−6.

(8) Mitsudome, T.; Mikami, Y.; Funai, H.; Mizugaki, T.; Jitsukawa, K.; Kaneda, K. *Angew. Chem.* **2008**, *120*, 144−147; *Angew. Chem., Int. Ed.* **2008**, *47*, 138−141.

(9) Mitsudome, T.; Mikami, Y.; Ebata, K.; Mizugaki, T.; Jitsukawa, K.; Kaneda, K. *Chem. Commun.* **2008**, 4804−4806.

(10) Kissin, Y. V. *Alkene Polymerization Reactions with Transition Metal Catalysts*; Elsevier: Amsterdam, 2008.

(11) Gary, J. H.; Handwerk, G. E. *Petroleum Refining Technology and Economics*; 2nd ed.; Marcel Dekker, Inc.: New York, 1984; ISBN 0-8247-7150-8.

(12) Smil, V. *Enriching the Earth: Fritz Haber, Carl Bosch, and the Transformation of World Food Production*: MIT Press: Cambridge, MA; 2001; ISBN 0-262-19449-X.

(13) Jin, R. *Nanotechnol. Rev.* **2012**, *1*, 31−56.

(14) Astruc, D. Transition-Metal Nanoparticles in Catalysis: From Historical Background to the State-of-the Art. In *Nanoparticles and Catalysis*; Astruc, D., Ed.; Wiley-VCH Verlag & Co.: Weinheim, Germany, 2008; pp 1−48.

(15) Wang, Q.; Ostafin, A. E. Metal Nanoparticles in Catalysis. In *Encyclopedia of Nanoscience and Nanotechnology*; Nalwa, H. S., Ed.; American Scientific Publishers: Stevenson Ranch, CA, 2004; Vol *5*, pp 475−503.

(16) Cushing, B. L.; Kolesnichenko, V. L.; O'Connor, C. J. *Chem. Rev.* **2004**, *104*, 3893−3946.

(17) Davis, S. C.; Klabunde, K. J. *Chem. Rev.* **1982**, *82*, 153−208.

(18) Barbaro, P.; Dal Santo, V.; Liguori, F. *Dalton Trans.* **2010**, *39*, 8391−8402.

(19) Piera, J.; Bäckvall, J.-E. *Angew. Chem.* **2008**, *120*, 3558−3576; *Angew. Chem., Int. Ed.* **2008**, *47*, 3506−3523.

(20) Haruta, M.; Yamada, N.; Kobayashi, T.; Iijima, S. *J. Catal.* **1989**, *115*, 301−309.

(21) Grirrane, A.; Corma, A.; Garcia, H. *Science* **2008**, *322*, 1661−1664.

(22) Gross, E.; Krier, J. M.; Heinke, L.; Somorjai, G. A. *Top. Catal.* **2012**, *55*, 13−23.

(23) Somorjai, G. A.; Li, Y. M. *Top. Catal.* **2010**, *53*, 832−847.

(24) Wang, D.; Xie, T.; Peng, Q.; Li, Y. *J. Am. Chem. Soc.* **2008**, *130*, 4016−4022.

(25) Wang, X.; Zhuang, J.; Peng, Q.; Li, Y. *Nature* **2005**, *437*, 121−124.

(26) Wang, D.; Peng, Q.; Li, Y. *Nano Res.* **2010**, *3*, 574−580.

(27) Hunger, K. *Industrial Dyes: Chemistry, Properties, Applications*; Wiley-VCH: Weinheim, 2003.

(28) Hoult, J. R. S. *Drugs* **1986**, *32*, 18−26.

(29) Kuwabara, T.; Nakajima, H.; Nanasawa, M.; Ueno, A. *Anal. Chem.* **1999**, *71*, 2844−2849.

(30) Stick, R. V.; Mocerino, M.; Franz, D. A. *J. Chem. Educ.* **1996**, *73*, 540−541.

(31) Orbán, M.; Kurin-Csörgei, K.; Zhabotinsky, A. M.; Epstein, I. R. *J. Am. Chem. Soc.* **1998**, *120*, 1146−1150.

(32) Pratt, E. F.; McGovern, T. P. *J. Org. Chem.* **1964**, *29*, 1540−1543.

(33) Baer, E.; Tosoni, A. L. *J. Am. Chem. Soc.* **1956**, *78*, 2857−2858.

(34) Orito, K.; Hatakeyama, T.; Takeo, M.; Uchiito, S.; Tokuda, M.; Suginome, H. *Tetrahedron* **1998**, *54*, 8403−8410.

(35) Zhang, C.; Jiao, N. *Angew. Chem.* **2010**, *122*, 6310−6313; *Angew. Chem., Int. Ed.* **2010**, *49*, 6174−6177.

(36) Dabbagh, H. A.; Teimouri, A.; Chermahini, A. N. *Dyes Pigm.* **2007**, *73*, 239−244.

(37) Barbero, M.; Cadamuro, S.; Dughera, S.; Giaveno, C. *Eur. J. Org. Chem.* **2006**, 4884−4890.

(38) Haghbeen, K.; Tan, E. W. *J. Org. Chem.* **1998**, *63*, 4503−4505.

(39) Davey, M. H.; Lee, V. Y.; Miller, R. D.; Marks, T. J. *J. Org. Chem.* **1999**, *64*, 4976−4979.

(40) Nutting, W. H.; Jewell, R. A.; Rapoport, H. *J. Org. Chem.* **1970**, *35*, 505−508.
(41) Sumesh, E.; Bootharaju, M. S.; Pradeep, A. T. *J. Hazard. Mater.* **2011**, *189*, 450−457.
(42) Lai, Y.; Zhang, H.; Xie, K.; Gong, D.; Tang, Y.; Sun, L.; Lin, C.; Chen, Z. *New J. Chem.* **2010**, *34*, 1335−1340.
(43) Zhang, J.; Wang, X.; Zhao, B.; Li, C. *Chem. Lett.* **2006**, *35*, 40−41.
(44) Sakai, H.; Kanda, T.; Shibata, H.; Ohkubo, T.; Abe, M. *J. Am. Chem. Soc.* **2006**, *128*, 4944−4945.
(45) Bhatte, K. D.; Tambade, P. J.; Dhake, K. P.; Bhanage, B. M. *Catal. Commun.* **2010**, *11*, 1233−1237.
(46) Domínguez-Vera, J. M.; Gálvez, N.; Sánchez, P.; Mota, A. J.; Trasobares, S.; Hernández, J. C.; Calvino, J. J. *Eur. J. Inorg. Chem.* **2007**, 4823−4826.
(47) Giuffrida, S.; Ventimiglia, G.; Sortino, S. *Chem. Commun.* **2009**, *27*, 4055−4057.
(48) Cong, H.; Porco, J. A., Jr. *ACS Catal.* **2012**, *2*, 65−70.